

Liquid Crystallinity and Organogelation Behavior of Lignin-Derived Metabolic Intermediate Bearing Cholesterol Groups

Tsuyoshi Michinobu,^{*1,2} Kenta Hiraki,¹ Nozomu Fujii,¹ Kazuhiro Shikinaka,¹ Yoshihiro Katayama,^{3,†} Eiji Masai,⁴ Masaya Nakamura,⁵ Yuichiro Otsuka,⁵ Seiji Ohara,⁵ and Kiyotaka Shigehara^{*1}

¹Graduate School of Engineering and Institute of Symbiotic Science and Technology, Tokyo University of Agriculture and Technology, Koganei, Tokyo 184-8588

²Global Edge Institute, Tokyo Institute of Technology, Ookayama, Meguro-ku, Tokyo 152-8550

³Graduate School of Bio-Applications and Systems Engineering, Tokyo University of Agriculture and Technology, Koganei, Tokyo 184-8588

⁴Department of Bioengineering, Nagaoka University of Technology, Nagaoka, Niigata 940-2188

⁵Forestry and Forest Products Research Institute, Tsukuba, Ibaraki 305-8687

Received February 21, 2011; E-mail: michinobu.t.aa@m.titech.ac.jp, jun@cc.tuat.ac.jp

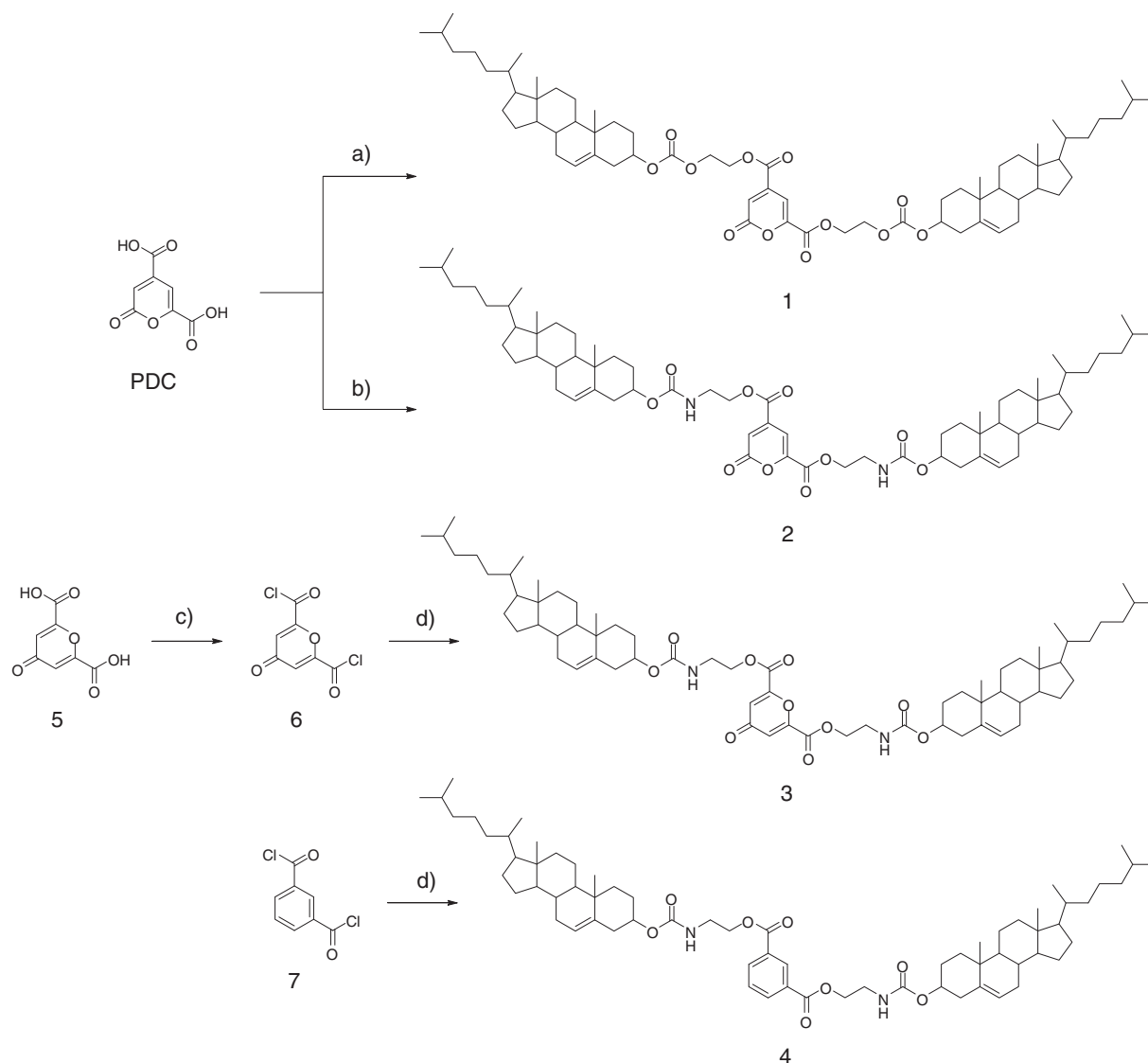
Two cholesterol groups were for the first time attached to a lignin-derived metabolic intermediate, 2-pyrone-4,6-dicarboxylic acid (PDC). This PDC molecule showed a liquid crystalline mesophase and interesting organogelation behavior. The relationship between molecular structure and assembly properties was investigated by modifying the PDC core and a spacer group between the PDC and cholesterol moieties. Although all derivatives displayed similar phase transition behavior with a SmA phase, only a few of them could form organogels. Detailed morphology investigations of the xerogels by X-ray diffraction (XRD) and scanning electron microscopy (SEM) suggested that both the PDC moiety and a carbamate spacer are essential for the occurrence of organogelation. Hydrogen bonds of the carbamate spacers and van der Waals interactions of the cholesterol moieties lead to a dipolar-induced interaction of the pyrone rings. The physical gels were probably stabilized by these cooperative interactions. The IR and ¹HNMR spectroscopies clearly revealed the presence of weak intermolecular interactions, such as hydrogen bonds and dipolar-type interactions, for efficient gelator molecules.

Synthetic cholesterol derivatives have been employed as versatile soft materials that display liquid crystallinity, organogelation properties, and chiral recognition ability based on molecular assembling features.¹ These significant properties usually originate from the cholesterol moieties. For example, cholesterol-substituted diacetylene compounds often form stable gels in nonpolar solvents. Introduction of carbamate spacers into these compounds enables the improvement of gel stability as well as the photopolymerization of the diacetylene moieties.^{1c} Recently, it was also shown that Langmuir monolayers of cholesterol-armed cyclen complexes become a platform for excellent enantioselective recognition of amino acids in response to lateral mechanical forces.² In order to achieve the chiral recognition abilities, it is important to carefully design the chemical structures of host molecules so that the chiral carbon atoms of the cholesterol moieties can become effective recognition sites. Both of these examples suggested that cholesterol-derived properties largely depend on other components attached to the cholesterol moieties.

We have, in the past several years, been involved in lignin-derived functional polymers and materials. The key substance in

this project has been 2-pyrone-4,6-dicarboxylic acid (PDC) (IUPAC recommended name: 2-oxo-2H-pyran-4,6-dicarboxylic acid), which was prepared from lignin biometabolic intermediates by a transformed bacterium.³ The X-ray crystal structure of PDC revealed an unusually short intermolecular hydrogen-bond due to the interactions between the highly polarized carbonyl groups of the pyrone ring.⁴ In addition, because PDC possesses two carboxylic acid groups, it can serve as a bifunctional monomer for polycondensation and polyaddition.⁵ The biomass-based polyesters containing PDC units displayed better thermal stabilities than conventional bio-based polyesters, such as poly(L-lactic acid) (PLLA).⁶ These thermal improvements are due to the strong interactions between the pseudo-aromatic rings integrated into the polymers. Therefore, we became interested in combining PDC with cholesterol moieties, which is expected to produce interesting assembly behavior. It should also be noted that preparation of biomass-based functional materials is of great importance to create a carbon-neutral society.⁷ In this paper, we report the synthesis of cholesterol-appended PDC derivatives.^{8,9} The assembly behavior of these molecules was elucidated by the liquid crystallinity and organogelation behavior. The effect of the PDC moiety was also evaluated by comparison to the derivatives of a symmetric PDC isomer, 4-oxo-4H-pyran-2,6-dicarboxylic acid, and isophthalic acid.

[†] Present address: College of Bioresource Science, Nihon University, Fujisawa, Kanagawa 252-0880



Scheme 1. Synthesis of dicholesterol-substituted derivatives: a) Cholest-5-en-3-yl 2-hydroxyethyl carbonate, DIC, DMAP, THF, 20 °C, 1 h, 40%; b) cholest-5-en-3-yl (2-hydroxyethyl)carbamate, DIC, DMAP, THF, 20 °C, 1 h, 46%; c) SOCl₂, BzEt₃NCl, 1,2-dichloroethane, 80 °C, 2.5 h, 81%; d) cholest-5-en-3-yl (2-hydroxyethyl)carbamate, DMAP, NEt₃, CH₂Cl₂, 0 → 20 °C, 11 h, 39% for **3**, 54% for **4**.

Results and Discussion

Synthesis of Cholesterol Derivatives. In the course of the previous synthetic studies of PDC derivatives, we found that PDC is unstable under basic conditions.^{5a} Based on this prerequisite, cholesterol-appended PDC derivatives, bis(2-[(cholest-5-en-3-yloxy)carbonyl]oxy)ethyl 2-oxo-2H-pyran-4,6-dicarboxylate (**1**) and bis(2-[(cholest-5-en-3-yloxy)carbonyl]amino)ethyl 2-oxo-2H-pyran-4,6-dicarboxylate (**2**), were newly synthesized from PDC by condensation with hydroxylated cholesterol derivatives using 4-(dimethylamino)pyridine (DMAP) and diisopropylcarbodiimide (DIC) in 40–46% yield (Scheme 1). The purity of the products was confirmed by HPLC analyses, and the chemical structures were unambiguously characterized by ¹H- and ¹³CNMR, FT-IR, MALDI-TOF-MS, and elemental analysis. A functionalization of a

symmetric PDC isomer, 4-oxo-4H-pyran-2,6-dicarboxylic acid (**5**), was also attempted using the hydroxylated cholesterol derivative. In this case, **5** was first converted into the corresponding acid chloride **6** in 81% yield. The reaction of **6** with 2 equiv of cholest-5-en-3-yl (2-hydroxyethyl)carbamate then yielded the desired product **3** in 39%. In a similar way, another model compound **4** was synthesized from isophthaloyl dichloride (**7**) in 45%. These cholesterol derivatives were also characterized by the common spectroscopic methods described above.

Phase Transition Behavior. The dicholesterol derivatives **1–4** were subjected to thermogravimetric analysis (TGA). The PDC derivatives **2** and **3** with carbamate spacers displayed onset decomposition temperatures of ca. 210 °C under nitrogen flow (Figure 1). Replacement of the carbamate spacer by a carbonate or the pyrone ring by a phenylene ring improved the thermal stability, and accordingly **1** and **4** showed an onset

decomposition temperature of ca. 270 °C under the same conditions. The 5% decomposition temperatures of **1–4** are 280, 239, 229, and 275 °C, respectively.

Based on the TGA results, the phase behavior of **1–4** was studied using differential scanning calorimetry (DSC) in a temperature range of less than the onset decomposition temperatures. The phase transition temperatures were estimated from the second heating scan of the DSC thermograms. All compounds showed a transition from a glass state to a liquid crystalline mesophase at 75–92 °C (Table 1). The mesophases of all compounds were determined to be smectic A from the polarized optical microscopy (POM) images (Figure 2 insets) and the X-ray diffraction (XRD) patterns (Figure 2). The XRD patterns provided layer distances of 4.36 nm for **1**, 4.46 nm for **2**, 4.18 nm for **3**, and 4.57 nm for **4**, which most likely correspond to the single molecular sizes. Further heating of the

mesophases induced a transition to an isotropic phase at 167 °C for **1** and 177 °C for **4**, while the mesophases of **2** and **3** were retained up to their decomposition temperatures. These results suggest that the combination of PDC core and carbamate spacers enhances intermolecular interactions.

Gelation Behavior. Organogelation properties of all compounds were investigated for 14 different solvents at various concentrations (Table 2). It was revealed that a carbamate spacer is essential for gelation of organic solvents, because **1** with a carbonate spacer did not form gels with any solvent. Therefore, the detailed investigations were performed using three other cholesterol derivatives **2–4** with a carbamate spacer. The results summarized in Table 2 suggest that the pyrone rings are also absolutely necessary for the occurrence of organogelation. The asymmetric PDC derivative **2** exhibited excellent gelation ability for benzene, cyclohexane, hexane, and ligroin, while the symmetric PDC derivative **3** showed similar gelation behavior for cyclohexane, ligroin, and tetrachloromethane. Although the number of the solvents gelled by **2** was greater than that by **3**, the symmetric PDC **3** could usually form gels more smoothly than **2**. In other words, it is

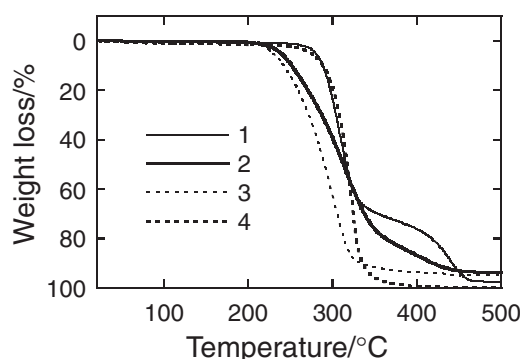


Figure 1. TGA curves of **1–4** at the heating rate of 10 °C min^{−1} under nitrogen.

Table 1. Phase Transition Behavior of **1–4**^{a)}

	Transition temperature/°C
1	G 75 SmA 167 Iso.
2	G 87 SmA 218 Dec.
3	G 92 SmA 210 Dec.
4	G 84 SmA 177 Iso.

a) Determined by the second heating cycle of DSC thermograms. G, glass; SmA, smectic A; Iso., isotropic; Dec., decomposition.

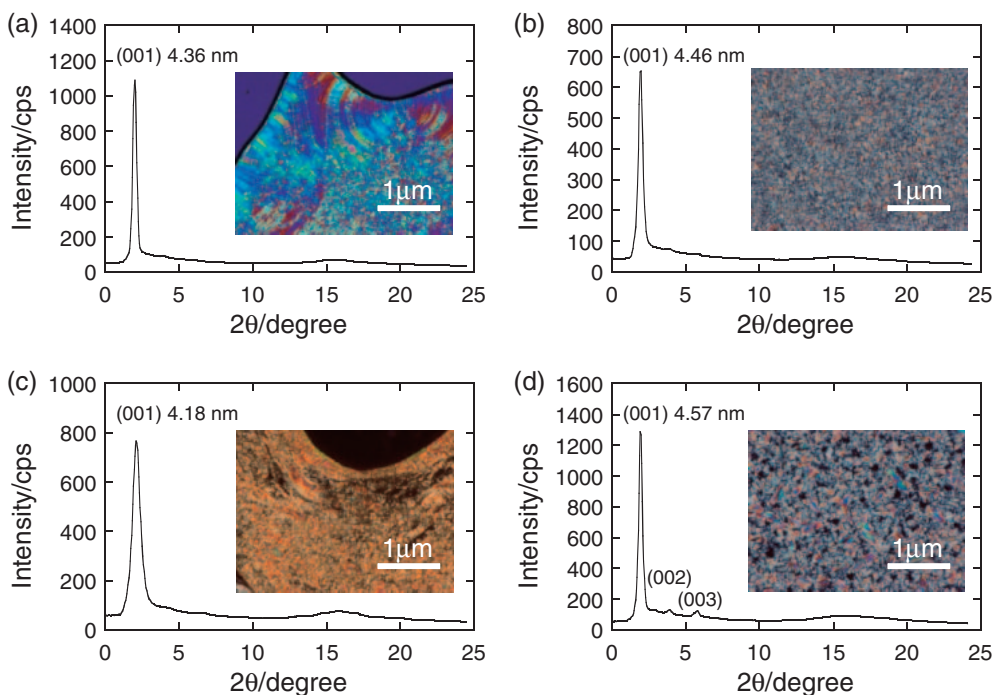


Figure 2. XRD patterns and POM images of (a) **1**, (b) **2**, (c) **3**, and (d) **4** at 140 °C.

Table 2. Gelation Test Results of **2–4** Using Various Organic Solvents^{a)}

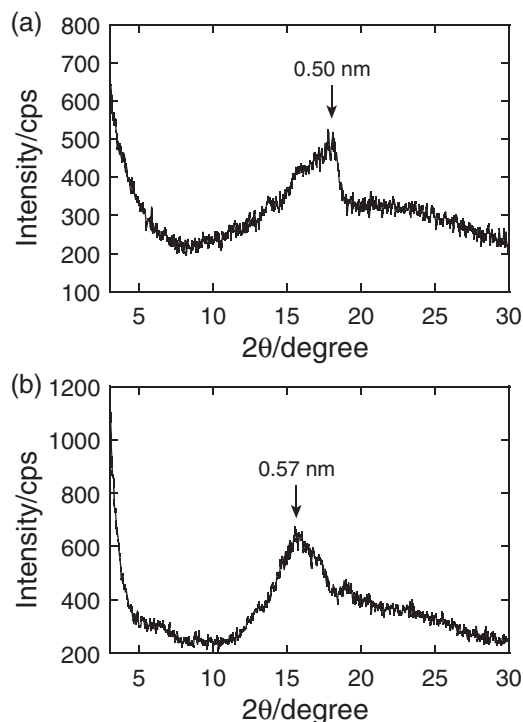
Solvent	2	3	4
Acetone	P	I	P
Acetonitrile	I	I	I
Benzene	G (7.4)	PG	S
Chloroform	S	S	S
Cyclohexane	G (4.1)	G (4.1)	S
Dichloromethane	S	S	S
Diethyl ether	P	I	P
Disopropyl ether	PG	PG	S
Ethanol	I	I	S
Ethyl acetate	I	I	S
Hexane	G (10)	I	P
Ligroin	G (3.7)	G (7.6)	P
Tetrachloromethane	S	G (2.1)	S
THF	S	S	S

a) S, soluble; I, insoluble; P, precipitated; PG, partial gel; G, gel. Critical gelation concentrations (wt %) are designated in parentheses.

**Figure 3.** Photograph of the cyclohexane gel of **2** (4.1 wt %) in an NMR tube at 20 °C.

thought that the gelation by **3** occurs through kinetic processes, while that by **2** is mainly governed by thermodynamic factors. For example, the gel of **3** and cyclohexane resulted within 3 min at 20 °C, while that of **2** and cyclohexane required overnight. A typical cyclohexane gel is shown in Figure 3. These gels were so thermally and physically stable that they did not show any gel–sol transitions up to the boiling point of cyclohexane (81 °C). The critical gelation concentrations were also estimated by concentration-dependent experiments. The most efficient gel formation was achieved from a ligroin solution for **2** (3.7 wt %) and a tetrachloromethane solution in the case of **3** (>2.1 wt %).

Because the cyclohexane gels of **2** and **3** showed the same critical gelation concentration, comparison of their analyzed data was expected to provide detailed information about the individual assembly forms. Thus, the xerogels prepared by freeze-drying the cyclohexane gels of **2** and **3** were investigated by XRD analysis and scanning electron microscopy (SEM). The XRD analysis of the xerogels of **2** and **3** indicated a broad but well-defined peak at $2\theta = 17.8$ ($d = 0.50$ nm) and 15.6° ($d = 0.57$ nm), respectively (Figure 4). The d -spacing values were independent of the gelator concentrations, suggesting that

**Figure 4.** XRD patterns of the xerogels of (a) **2** and (b) **3** prepared at the concentration of 8.2 wt % in cyclohexane.

the gelation always occurs in the same assembly process. These distances also indicated the presence of organized short intermolecular distances for the xerogels of both **2** and **3**. The slight difference in the d -spacing values would be caused by the different pyrone rings. However, no noticeable differences were observed when SEM images were taken. The cyclohexane xerogels of both **2** and **3** revealed the formation of a layered flake-like structure, implying that the molecular assembly modes with cyclohexane were basically the same (Figures 5a and 5b). On the other hand, when the gelation solvent of **3** was changed from cyclohexane into tetrachloromethane, a completely different morphology resulted (Figure 5c). The dense belt-like morphology of the tetrachloromethane xerogel clearly represents a more efficient gelation ability compared to the cyclohexane gel. These xerogel morphologies are often observed and explained by a 2D organization of gelator molecules in terms of the intermolecular interactions with solvent molecules.¹⁰

In order to elucidate the weak intermolecular interactions, such as hydrogen bonds, FT-IR spectra of **2** and **3** were obtained in a CH_2Cl_2 solution and a cyclohexane gel at the same concentration (4.1 wt %). Characteristic peaks of the NH and C=O groups of the carbamate and PDC moieties were noted. In CH_2Cl_2 , the individual molecules are homogeneously dissolved and intermolecular interactions are negligible. Thus, the asymmetric PDC derivative **2** in CH_2Cl_2 displayed an almost free NH stretching band at 3446 cm^{-1} (Figure 6Aa). However, this band shifted to 3377 cm^{-1} in the cyclohexane gel, suggesting a hydrogen-bond formation (Figure 6Ab). Similar to this result, the C=O stretching band of the carbamate

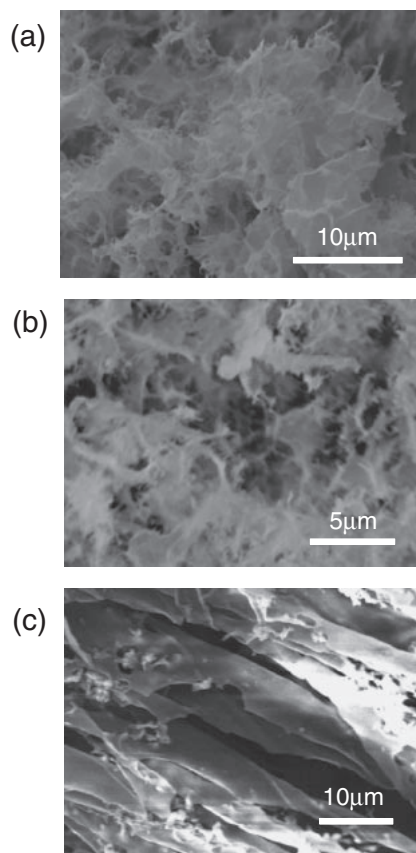


Figure 5. SEM images of the xerogels of (a) **2** prepared from cyclohexane at 4.1 wt %, (b) **3** prepared from cyclohexane at 4.1 wt %, and (c) **3** prepared from tetrachloromethane at 2.1 wt %.

moieties of **2** detected at 1716 cm^{-1} in CH_2Cl_2 shifted to a lower energy of 1698 cm^{-1} in the cyclohexane gel. These results are consistent with a previous report,¹¹ and accordingly these shifts are strong evidence for hydrogen-bond formations, which stabilize the assembled structure of **2** in a gel state. Furthermore, the C=O stretching bands of the 2-pyrone ring and ester moieties were partially overlapped at around 1740 cm^{-1} in CH_2Cl_2 . These bands were apparently split into two bands in the cyclohexane gel. The low energy shift to 1729 cm^{-1} is most likely associated with the dipolar interaction of the 2-pyrone ring, as reported previously.⁴ Similar IR spectra were obtained for the symmetric PDC derivative **3**. The free NH stretching band was detected at 3448 cm^{-1} in CH_2Cl_2 , while the cyclohexane gel exhibited new hydrogen-bonding bands in the lower energy region of $\approx 3300\text{ cm}^{-1}$ (Figure 6B). However, the presence of the original free NH stretching band in the cyclohexane gel suggests incomplete organization, despite the faster gelation ability than **2**. The C=O stretching band of the carbamate moieties of **3** also shifted from 1716 cm^{-1} in CH_2Cl_2 to 1702 cm^{-1} in the cyclohexane gel. In addition, the C=O stretching band ascribed to the dipolar-type interaction of the 4-pyrone ring was weakly detected at 1721 cm^{-1} in the gel state. This result again suggests the irregular organization of the **3**/cyclohexane gel compared to the isomeric **2**/cyclohexane gel.

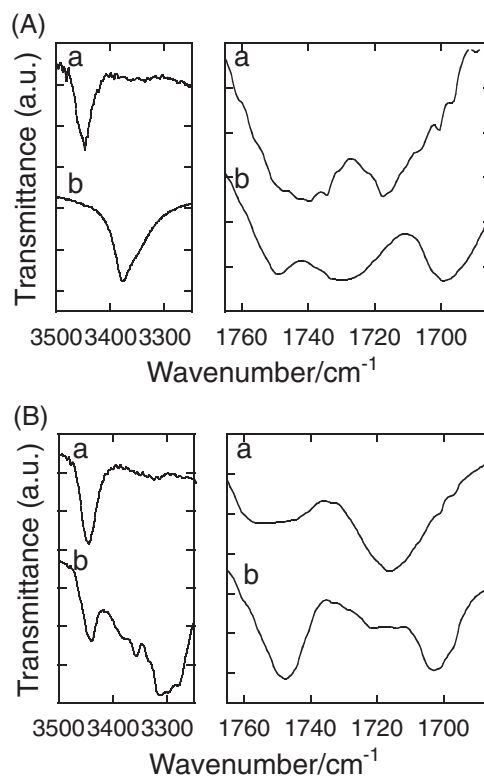


Figure 6. IR spectra of (A) **2** measured (a) in a CH_2Cl_2 solution (4.1 wt %) and (b) as a cyclohexane gel (4.1 wt %) and (B) **3** measured (a) in a CH_2Cl_2 solution (4.1 wt %) and (b) as a cyclohexane gel (4.1 wt %).

Self-assembly of **2–4** was further analyzed by ^1H NMR spectroscopy. All compounds showed good solubility in CDCl_3 , and the spectra did not show any concentration dependence in the measured range from 1 to 20 mM. Thus, temperature-dependent ^1H NMR spectra of **2** were measured in CDCl_3 at the concentration of 5 mM (ca. 3.7 wt %). The carbamate protons exhibited an upfield shift by ca. 0.02 ppm when heated from 25 to 55°C , suggesting the presence of hydrogen bonds.^{9f} The extent of the shift was more significant in the case of the PDC protons. The PDC moiety displayed a broad single peak and a doublet peak at 7.55 and 7.16 ppm, respectively, at 25°C (Figure 7a). The lower magnetic field peak is ascribed to the 5-position of the pyrone ring, while the higher magnetic field peak is derived from the 2-position. When the solution was gradually heated, both peaks started to shift to higher magnetic field, and the peak of the 5-position proton finally became a doublet peak (7.51 ppm) at 55°C . This clearly suggests that there is an intermolecular interaction between the pyrone rings at temperatures close to room temperature, even though the solvent did not show gelation behavior and the IR spectra in CH_2Cl_2 did not provide evidence for the pyrone ring interactions. A similar temperature-dependent behavior was observed for the symmetric PDC derivative **3**. The peak ascribed to the 3,5-positions of the pyrone ring shifted to a higher magnetic field, as the solution temperature increased (Figure 7b). The peak shape also became sharper

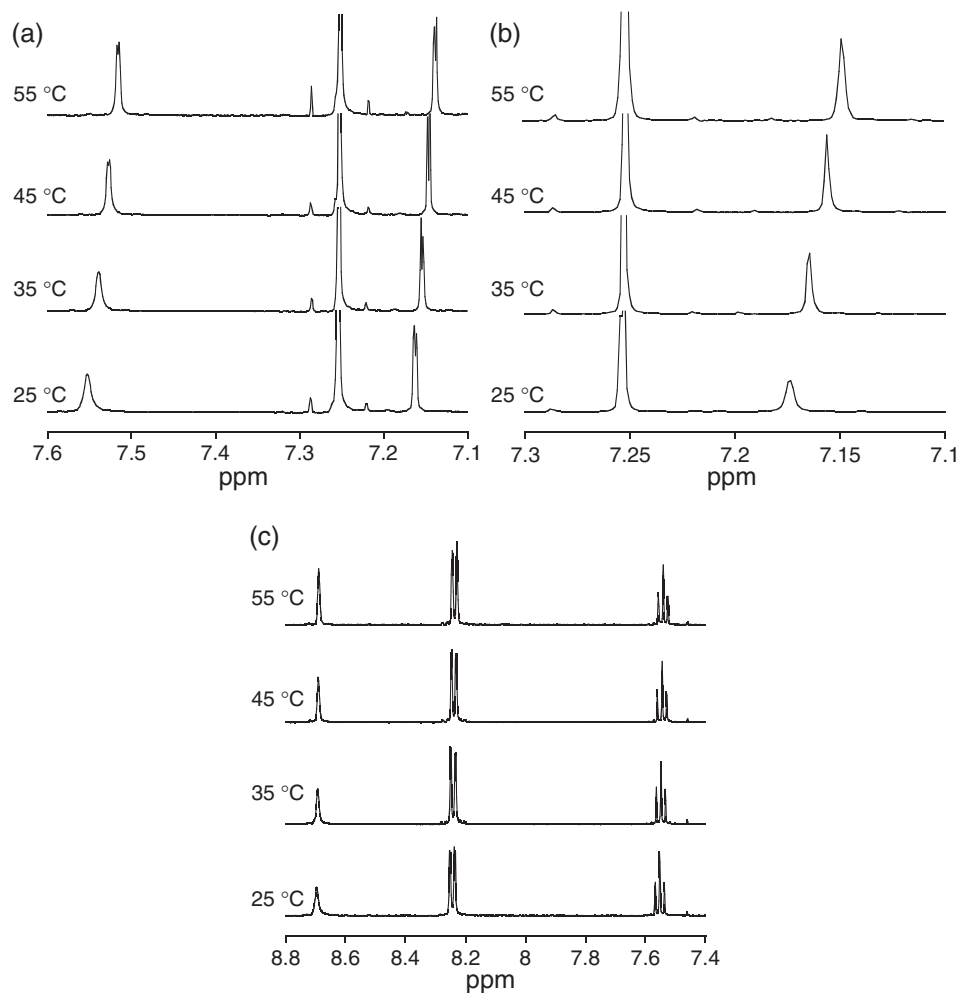


Figure 7. ^1H NMR spectra of (a) **2** [5 mM (3.7 wt %)], (b) **3** [5 mM (3.7 wt %)], and (c) **4** [5 mM (3.6 wt %)] in CDCl_3 at various temperatures.

upon heating. In contrast, there were few effects of heating on the phenylene protons of **4** (Figure 7c). These results most likely reflect the different self-assembly features of the (pseudo-)aromatic rings, which are associated with the organogelation behavior (vide supra).

The temperature-dependent ^1H NMR experiments clearly revealed the interactions between the PDC moieties. It is well-known that organogels are formed through the 1D alignment of gelator molecules in terms of van der Waals, dipole-dipole, π - π , and hydrogen-bonding interactions.¹² Based on the dipolar-induced interaction of the pyrone rings as well as the hydrogen bonds of the carbamate moieties revealed by the IR spectra, a structural model of the assembly modes is proposed (Figure 8). The dipolar-type antiparallel interactions of the pyrone rings are strengthened by the hydrogen bonds of the carbamate moieties and van der Waals interactions of the cholesterol moieties. Because the pyrone rings are pseudo-aromatic, several resonance structures can be drawn. The observed broadening of some ^1H NMR peaks was probably due to electron perturbations in terms of the pyrone ring interactions.

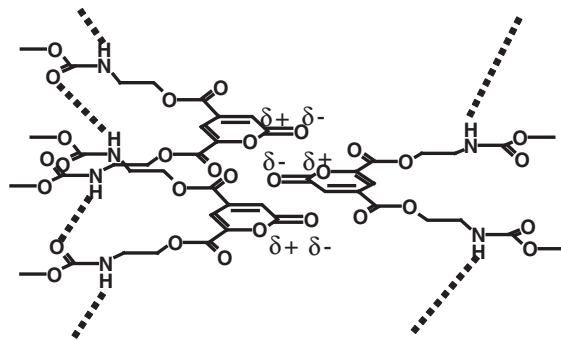


Figure 8. A presumed self-assembly model of **2**.

Conclusion

In conclusion, molecular assemblies of dicholesterol-appended PDC derivatives were examined. All derivatives displayed the SmA phase at elevated temperatures. However, the structural investigations revealed that the organogelation abilities are achieved only when both the PDC core and

carbamate spacers exist in a single molecule. Gels of apolar organic solvents, such as benzene, cyclohexane, hexane, and ligroin, were formed at the gelator concentration of 2.1–10 wt%. Both symmetric and asymmetric PDC derivatives displayed a similar morphology of the xerogels, as revealed by the XRD patterns and SEM images. Further investigations of the IR and temperature-dependent ^1H NMR spectra clearly demonstrated the intermolecular interactions, such as the hydrogen bonds of the carbamate moieties and the dipolar-induced interactions of the pyrone rings. It should be noted that replacement of the pyrone ring by a phenylene ring led to the significant decrease in the latter intermolecular interactions, and accordingly no organogelation abilities resulted. All these results offer the design principles for biomass-based functional molecules and materials.

Experimental

Materials. All reagents and dehydrated solvents were purchased from Kanto, Tokyo Kasei, and Wako and used as received. 2-Pyrone-4,6-dicarboxylic acid (PDC) was prepared from protocatchuate via the metabolic pathway of *Sphingomonas paucimobilis* SYK-6.³ Cholest-5-en-3-yl 2-hydroxyethyl carbonate¹³ and cholest-5-en-3-yl (2-hydroxyethyl)carbamate¹⁴ were prepared from cholest-5-en-3-yl chloroformate according to literature methods.

Measurements. ^1H NMR and ^{13}C NMR spectra were measured on a JEOL model AL300 or AL400 spectrometer at 20 °C. Chemical shifts are reported in ppm downfield from SiMe_4 , using the solvent's residual signal as an internal reference. Infrared (IR) spectra were recorded on a JASCO FT/IR-4100 spectrometer. IR spectra of xerogels were measured on a KRS-5 plate. HPLC was measured on a JASCO system equipped with polystyrene gel columns using THF as an eluent at a flow rate of 1.0 mL min^{-1} . Thermogravimetric analysis (TGA) and differential scanning calorimetry (DSC) measurements were carried out on a Rigaku Thermoplus TG8120 and DSC8230, respectively, under flowing nitrogen at a scanning rate of $10\text{ }^\circ\text{C min}^{-1}$. Xerogels prepared by freeze-drying of the cyclohexane gel were analyzed using a JEOL JSM-6510 SEM. A glass slide was used as a substrate and a gold coating was performed. Wide-angle X-ray diffraction (WAXD) patterns of the xerogels were recorded by irradiating Ni-filtered $\text{Cu K}\alpha$ radiation with a Rigaku R472-C. Mesophase textures were observed with an Olympus BX51 polarized optical microscopy (POM) equipped with a hot stage. X-ray diffraction patterns of the mesophase were recorded by irradiating Ni-filtered $\text{Cu K}\alpha$ radiation with a Rigaku-Denki UltraX18.

Bis(2-[(cholest-5-en-3-yloxy)carbonyl]oxy)ethyl 2-Oxo-2H-pyran-4,6-dicarboxylate (1). To a dry THF solution (10 mL) of PDC (500 mg, 2.72 mmol) and cholest-5-en-3-yl 2-hydroxyethyl carbonate (2.58 g, 5.43 mmol), a dry THF solution (5 mL) of diisopropylcarbodiimide (DIC) (754 mg, 5.97 mmol) and 4-(dimethylamino)pyridine (DMAP) (16.5 mg, 0.135 mmol) was added dropwise at 20 °C. After stirring for 1 h at 20 °C, the precipitate was removed by filtration and the filtrate was evaporated. The crude product was dissolved in CH_2Cl_2 and washed with diluted aq. HCl and brine. After drying over MgSO_4 , column chromatography (SiO_2 , $\text{CHCl}_3/\text{CH}_3\text{OH}$ 35:1), followed by recrystallization from acetone

afforded the almost pure desired product. The white solid was then dissolved into CHCl_3 and precipitated into CH_3OH . The precipitate was collected and dried in vacuo at 50 °C (1.18 g, 40%).

Mp 165 °C; ^1H NMR (300 MHz, CDCl_3 , 298 K): δ 0.65–1.59 (m, 84H), 2.21–2.29 (m, 4H), 4.45–4.60 (m, 8H), 5.32 (s, 2H), 7.18 (d, $J = 1.5\text{ Hz}$, 1H), 7.53 (d, $J = 1.3\text{ Hz}$, 1H); ^{13}C NMR (100 MHz, CDCl_3 , 298 K): δ 11.81, 18.67, 19.21, 20.98, 22.52, 22.79, 23.78, 24.23, 27.58, 27.96, 28.18, 31.76, 31.84, 35.73, 36.12, 36.46, 36.74, 37.89, 39.45, 39.64, 42.25, 49.91, 56.07, 56.61, 64.13, 64.39, 64.49, 78.39, 108.48, 123.01, 123.11, 139.04, 139.14, 142.38, 149.07, 154.18, 158.62, 159.23, 162.06; IR (KBr): ν 2950, 2867, 1744, 1559, 1467, 1375, 1332, 1247, 1169, 1107, 1028, 994, 972, 946, 889, 791, 761, 668 cm^{-1} ; MALDI-TOF-MS (matrix: dithranol): m/z : calcd for $\text{C}_{67}\text{H}_{100}\text{O}_{12}\text{Na}^+$: 1120.5; found: 1120.1 $[\text{M} + \text{Na}]^+$.

Bis(2-[(cholest-5-en-3-yloxy)carbonyl]amino)ethyl 2-Oxo-2H-pyran-4,6-dicarboxylate (2). In a similar way to **1**, the reaction of PDC and cholest-5-en-3-yl (2-hydroxyethyl)carbamate yielded **2** (46%) as a white solid.

Mp 218.3 °C (decomposition); ^1H NMR (300 MHz, CDCl_3 , 298 K): δ 0.65–2.01 (m, 82H), 2.27–2.35 (m, 4H), 3.56 (br s, 4H), 4.39–4.49 (m, 6H), 4.97–5.06 (m, 2H), 5.35 (s, 2H), 7.16 (s, 1H), 7.55 (s, 1H); ^{13}C NMR (75 MHz, CDCl_3 , 298 K): δ 11.82, 18.67, 19.29, 21.00, 22.53, 22.79, 23.81, 24.25, 27.97, 28.07, 28.19, 31.81, 31.85, 35.76, 36.15, 36.50, 36.90, 38.46, 39.48, 39.68, 42.26, 49.95, 56.10, 56.63, 66.09, 74.78, 97.12, 108.58, 122.91, 142.78, 149.24, 156.15, 158.76, 159.41, 162.17; IR (KBr): ν 3381, 2949, 1733, 1520, 1466, 1332, 1241, 1117, 1031, 761 cm^{-1} ; MALDI-TOF-MS (matrix: dithranol): m/z : calcd for $\text{C}_{67}\text{H}_{102}\text{N}_2\text{O}_{10}\text{Na}^+$: 1118.5; found: 1118.1 $[\text{M} + \text{Na}]^+$.

Bis(2-[(cholest-5-en-3-yloxy)carbonyl]amino)ethyl 4-Oxo-4H-pyran-2,6-dicarboxylate (3). To a solution of cholest-5-en-3-yl (2-hydroxyethyl)carbamate (3.15 g, 6.65 mmol), DMAP (77.4 mg, 0.635 mmol), and triethylamine (0.967 g, 9.56 mmol) in CH_2Cl_2 (26 mL), a solution of **6** (670 mg, 3.03 mmol) in CH_2Cl_2 (18 mL) was slowly added at 0 °C for 5 min. After stirring at 0 °C for 1 h, the mixture was warmed to 20 °C and stirred for 11 h. The mixture was washed with diluted aq. HCl followed by brine, then dried over Na_2SO_4 . After filtration, the filtrate was evaporated in vacuo. Column chromatography (SiO_2 , $\text{CHCl}_3/\text{CH}_3\text{OH}$ 20:1) followed by recrystallization from acetone afforded the white solid. This solid was further dissolved into CHCl_3 , which was reprecipitated into CH_3OH . The precipitate was collected and dried in vacuo at 75 °C, yielding **3** (1.31 g, 39%).

Mp 255 °C (decomposition); ^1H NMR (400 MHz, CDCl_3 , 298 K): δ 0.67–2.00 (m, 82H), 2.26–2.32 (m, 4H), 3.57 (d, $J = 4\text{ Hz}$, 4H), 4.41–4.46 (m, 6H), 5.03 (br s, 2H), 5.35–5.36 (m, 2H), 7.17 (s, 2H); ^{13}C NMR (100 MHz, CDCl_3 , 298 K): δ 11.83, 18.69, 19.29, 21.00, 22.53, 22.79, 23.82, 24.25, 27.97, 28.07, 28.19, 31.86, 35.77, 36.16, 36.51, 36.94, 38.48, 39.48, 39.70, 42.28, 49.98, 56.12, 56.64, 64.66, 74.60, 122.52, 128.70, 130.35, 130.88, 134.09, 139.69, 156.17, 165.60; IR (KBr): ν 3381, 2948, 1725, 1523, 1466, 1378, 1232, 1138, 1031, 730 cm^{-1} ; MALDI-TOF-MS (matrix: dithranol): m/z : calcd for $\text{C}_{68}\text{H}_{104}\text{N}_2\text{O}_8\text{Na}^+$: 1100.55; found: 1100.2 $[\text{M} + \text{Na}]^+$.

Bis(2-[(cholest-5-en-3-yloxy)carbonyl]amino)ethyl) Benzene-1,3-dicarboxylate (4). In a similar way to **3**, the reaction of isophthaloyl dichloride and cholest-5-en-3-yl (2-hydroxyethyl)carbamate yielded **4** (54%) as a white solid.

Mp 186 °C; $^1\text{H NMR}$ (400 MHz, CDCl_3 , 298 K): δ 0.66–2.32 (m, 84H), 3.61 (d, $J = 4$ Hz, 4H), 4.41–4.42 (m, 6H), 5.09 (s, 2H), 5.32–5.34 (m, 2H), 7.55 (t, $J = 6$ Hz, 1H), 8.24 (d, $J = 6$ Hz, 2H), 8.70 (s, 1H); IR (KBr): ν 3393, 2948, 2867, 1718, 1661, 1507, 1457, 1375, 1233, 1120, 1031, 780, 668 cm^{-1} ; MALDI-TOF-MS (matrix: dithranol): m/z : calcd for $\text{C}_{67}\text{H}_{102}\text{N}_2\text{O}_{10}\text{Na}^+$: 1118.5; found: 1118.1 [$\text{M} + \text{Na}$] $^+$.

4-Oxo-4H-pyran-2,6-dicarbonyl Dichloride (6). To a solution of 4-oxo-4H-pyran-2,6-dicarboxylic acid (**5**) (500 mg, 2.72 mmol) and benzyltriethylammonium chloride (1.8 mg, 7.9 μmol) in 1,2-dichloroethane (5 mL), thionyl chloride (0.825 mL, 11.4 mmol) was added. The mixture was heated to 80 °C for 2.5 h. After cooling to 20 °C, the solvent was evaporated and the residual solid was purified by recrystallization from hexane. The crystals were collected and dried in vacuo, yielding **6** (485 mg, 81%).

$^1\text{H NMR}$ (300 MHz, CDCl_3): δ 7.34 (s, 2H); $^{13}\text{C NMR}$ (75 MHz, CDCl_3): δ 121.91, 152.78, 161.48, 177.68; IR (KBr): ν 3083, 1758, 1639, 1590, 1401, 1339, 1238, 1189, 1167, 1120, 1038, 983, 963, 909, 874, 856, 757, 720, 705, 535 cm^{-1} .

This work was supported, in part, by a Grant-in-Aid for Scientific Research and Special Coordination Funds for Promoting Science and Technology from MEXT, Japan. We thank Profs. J. Watanabe and M. Tokita (Tokyo Inst. Technol.) for the use of the X-ray diffractometer and Dr. K. Tsuchiya (Tokyo Univ. Agr. Technol.) for the HPLC measurements.

References

- a) Y.-C. Lin, R. G. Weiss, *Macromolecules* **1987**, *20*, 414. b) S. Shinkai, K. Murata, *J. Mater. Chem.* **1998**, *8*, 485. c) N. Tamaoki, S. Shimada, Y. Okada, A. Belaissoui, G. Kruk, K. Yase, H. Matsuda, *Langmuir* **2000**, *16*, 7545. d) K. J. C. van Bommel, A. Friggeri, S. Shinkai, *Angew. Chem., Int. Ed.* **2003**, *42*, 980. e) A. Ajayaghosh, V. K. Praveen, *Acc. Chem. Res.* **2007**, *40*, 644. f) H. Maeda, *Chem.—Eur. J.* **2008**, *14*, 11274. g) G. O. Lloyd, J. W. Steed, *Nat. Chem.* **2009**, *1*, 437. h) D. K. Smith, *Chem. Soc. Rev.* **2009**, *38*, 684. i) M. Suzuki, K. Hanabusa, *Chem. Soc. Rev.* **2009**, *38*, 967. j) A. Dawn, T. Shiraki, S. Haraguchi, S.-i. Tamaru, S. Shinkai, *Chem. Asian J.* **2011**, *6*, 266.
- a) T. Michinobu, S. Shinoda, T. Nakanishi, J. P. Hill, K. Fujii, T. N. Player, H. Tsukube, K. Ariga, *J. Am. Chem. Soc.* **2006**, *128*, 14478. b) K. Ariga, T. Michinobu, T. Nakanishi, J. P. Hill, *Curr. Opin. Colloid Interface Sci.* **2008**, *13*, 23. c) T. Mori, K. Okamoto, H. Endo, J. P. Hill, S. Shinoda, M. Matsukura, H. Tsukube, Y. Suzuki, Y. Kanekiyo, K. Ariga, *J. Am. Chem. Soc.* **2010**, *132*, 12868. d) T. Michinobu, S. Shinoda, T. Nakanishi, J. P. Hill, K. Fujii, T. N. Player, H. Tsukube, K. Ariga, *Phys. Chem. Chem. Phys.* **2011**, *13*, 4895.
- Y. Otsuka, M. Nakamura, K. Shigehara, K. Sugimura, E. Masai, S. Ohara, Y. Katayama, *Appl. Microbiol. Biotechnol.* **2006**, *71*, 608.
- T. Michinobu, M. Bito, Y. Yamada, Y. Katayama, K. Noguchi, E. Masai, M. Nakamura, S. Ohara, K. Shigehara, *Bull. Chem. Soc. Jpn.* **2007**, *80*, 2436.
- a) T. Michinobu, Y. Inazawa, K. Hiraki, Y. Katayama, E. Masai, M. Nakamura, S. Ohara, K. Shigehara, *Chem. Lett.* **2008**, 37, 154. b) M. Hishida, K. Shikina, Y. Katayama, S. Kajita, E. Masai, M. Nakamura, Y. Otsuka, S. Ohara, K. Shigehara, *Polym. J.* **2009**, *41*, 297. c) T. Michinobu, M. Bito, M. Tanimura, Y. Katayama, E. Masai, M. Nakamura, Y. Otsuka, S. Ohara, K. Shigehara, *Polym. J.* **2009**, *41*, 843. d) T. Michinobu, M. Bito, Y. Yamada, M. Tanimura, Y. Katayama, E. Masai, M. Nakamura, Y. Otsuka, S. Ohara, K. Shigehara, *Polym. J.* **2009**, *41*, 1111. e) M. Hishida, K. Shikina, Y. Inazawa, Y. Katayama, S. Kajita, E. Masai, M. Nakamura, Y. Otsuka, S. Ohara, K. Shigehara, *Kobunshi Ronbunshu* **2009**, *66*, 141. f) Y. Hasegawa, K. Shikina, Y. Katayama, S. Kajita, E. Masai, M. Nakamura, Y. Otsuka, S. Ohara, K. Shigehara, *Sen'i Gakkaishi* **2009**, *65*, 359. g) T. Michinobu, M. Bito, M. Tanimura, Y. Katayama, E. Masai, M. Nakamura, Y. Otsuka, S. Ohara, K. Shigehara, *J. Macromol. Sci., Part A: Pure Appl. Chem.* **2010**, *47*, 564.
- T. Michinobu, M. Hishida, M. Sato, Y. Katayama, E. Masai, M. Nakamura, Y. Otsuka, S. Ohara, K. Shigehara, *Polym. J.* **2008**, *40*, 68.
- a) A. J. Ragauskas, C. K. Williams, B. H. Davison, G. Britovsek, J. Cairney, C. A. Eckert, W. J. Frederick, Jr., J. P. Hallett, D. J. Leak, C. L. Liotta, J. R. Mielenz, R. Murphy, R. Templer, T. Tschaplinski, *Science* **2006**, *311*, 484. b) K. Shikina, N. Fujii, S. Egashira, Y. Murakami, M. Nakamura, Y. Otsuka, S. Ohara, K. Shigehara, *Green Chem.* **2010**, *12*, 1914.
- For a preliminary communication of this work, see: T. Michinobu, K. Hiraki, N. Fujii, K. Shikina, Y. Katayama, E. Masai, M. Nakamura, Y. Otsuka, S. Ohara, K. Shigehara, *Chem. Lett.* **2010**, 39, 400.
- For recent examples of dicholesterol gelators, see: a) K. Sugiyasu, N. Fujita, M. Takeuchi, S. Yamada, S. Shinkai, *Org. Biomol. Chem.* **2003**, *1*, 895. b) K. Sugiyasu, N. Fujita, S. Shinkai, *Angew. Chem., Int. Ed.* **2004**, *43*, 1229. c) S.-i. Kawano, N. Fujita, S. Shinkai, *J. Am. Chem. Soc.* **2004**, *126*, 8592. d) S.-i. Kawano, N. Fujita, S. Shinkai, *Chem.—Eur. J.* **2005**, *11*, 4735. e) J. Peng, K. Liu, X. Liu, H. Xia, J. Liu, Y. Fang, *New J. Chem.* **2008**, *32*, 2218. f) M. Xue, K. Liu, J. Peng, Q. Zhang, Y. Fang, *J. Colloid Interface Sci.* **2008**, *327*, 94. g) C. Vijayakumar, V. K. Praveen, A. Ajayaghosh, *Adv. Mater.* **2009**, *21*, 2059. h) S. Abraham, R. K. Vijayaraghavan, S. Das, *Langmuir* **2009**, *25*, 8507. i) L. Ma, W. A. Harrell, Jr., J. T. Davis, *Org. Lett.* **2009**, *11*, 1599.
- a) R. Davis, R. Berger, R. Zentel, *Adv. Mater.* **2007**, *19*, 3878. b) Y. Misawa, N. Koumura, H. Matsumoto, N. Tamaoki, M. Yoshida, *Macromolecules* **2008**, *41*, 8841. c) P. Dastidar, *Chem. Soc. Rev.* **2008**, *37*, 2699.
- J. Nagasawa, M. Kudo, S. Hayashi, N. Tamaoki, *Langmuir* **2004**, *20*, 7907.
- a) J. H. Jung, S. Shinkai, T. Shimizu, *Chem.—Eur. J.* **2002**, *8*, 2684. b) M. Yoshida, N. Koumura, Y. Misawa, N. Tamaoki, H. Matsumoto, H. Kawanami, S. Kazaoui, N. Minami, *J. Am. Chem. Soc.* **2007**, *129*, 11039. c) H. Maeda, Y. Haketa, T. Nakanishi, *J. Am. Chem. Soc.* **2007**, *129*, 13661. d) S. Yagai, M. Ishii, T. Karatsu, A. Kitamura, *Angew. Chem., Int. Ed.* **2007**, *46*, 8005. e) P. Xue, R. Lu, G. Chen, Y. Zhang, H. Nomoto, M. Takafuji, H. Ihara, *Chem.—Eur. J.* **2007**, *13*, 8231. f) Y. Kamikawa, T. Kato, *Langmuir* **2007**, *23*, 274. g) I. Hisaki, H. Shigemitsu, Y. Sakamoto, Y. Hasegawa, Y. Okajima, K. Nakano, N. Tohnai, M. Miyata, *Angew. Chem., Int. Ed.* **2009**, *48*, 5465.
- H.-D. Tang, Y. Xiong, X.-L. Zhang, *Wuhan Univ. J. Nat. Sci.* **2000**, *5*, 233.
- C. Guisado, J. E. Waterhouse, W. S. Price, M. R. Jorgensen, A. D. Miller, *Org. Biomol. Chem.* **2005**, *3*, 1049.